

RESEARCH

Open Access

# Enhancement of ruthenium-promoted Co/CNT nanocatalyst performance using microemulsion technique

Ahmad Tavasoli\*, Somayeh Taghavi, Saber Tabyar and Saba Karimi

## Abstract

**Background:** Ruthenium-promoted cobalt nanocatalysts that are supported by carbon nanotubes (CNTs) are prepared using impregnation and microemulsion techniques. Ruthenium loadings were varied from 0 to 1 wt.% while the amount of cobalt was fixed at 15 wt.%. The nanocatalysts were extensively characterized by different methods and their activity and selectivity in Fischer-Tropsch synthesis (FTS) have been assessed in a fixed-bed microreactor. The physicochemical properties and performance of the nanocatalysts were compared with the catalyst prepared by impregnation method.

**Results:** Very narrow particle size distribution has been produced by the microemulsion technique. According to the transmission electron microscopy, pictures small Co particles (2 to 7 nm) are mostly confined inside the CNTs. Ruthenium increased the percentage reduction of the unpromoted catalyst by a factor of 25. Compared with the catalysts prepared by impregnation, using microemulsion technique with water-to-surfactant ratio of 0.5 which decreased the average cobalt oxide particle sizes to 4.8 nm, the percentage of dispersion is almost doubled and the percentage of reduction is increased by 28.

**Conclusions:** Addition of ruthenium increased the percentage conversion and  $C_5^+$  selectivity of the unpromoted catalyst by a factor of 22.6 and 7, respectively. Activity and selectivity were found to be dependent on the catalyst preparation method and water-to-surfactant ratio (as well as on cobalt particle sizes). The percentage of CO conversion and FTS rate increased from 59.09 to 75.05 and 0.291 to 0.372 gr HC/gr cat/h, respectively, while the  $C_5^+$  liquid hydrocarbons selectivity decreased slightly.

**Keywords:** Fischer-Tropsch synthesis, Cobalt, Ruthenium, Microemulsion, Particle size

## Background

Fischer-Tropsch (FT) synthesis is an alternative route for the production of transportation fuels from natural gas. Regardless of the operating conditions, FT synthesis always produces a wide range of light gases and distillates, including olefins, paraffins, and oxygenated products. Cobalt-based catalysts are preferentially applied in FTS processes aimed at producing precursors of the synthetic diesel owing to their high selectivity towards long-chain normal paraffins, their remarkable stability, and their lower activity for the competing water-gas shift reaction

(WGSR) as compared to alternative catalysts based on iron [1-3].

For cobalt catalysts supported by  $Al_2O_3$ ,  $SiO_2$ , and  $TiO_2$ , it has been shown that noble metals such as ruthenium are typically used to decrease the reduction temperature of the cobalt oxides and increase the dispersion of the cobalt clusters. Ru increases the number of active surface  $Co^0$  sites available for FT reaction in Ru-promoted catalysts and hence enhances the percentage of CO conversion and FTS reaction rate. Ru is more selective towards higher molecular weight hydrocarbons than cobalt. Therefore, the improvement in  $C_5^+$  selectivity observed for Ru-promoted catalysts as compared to unpromoted catalyst may be due to the Ru enrichment on the cobalt crystallite surface [4,5].

\* Correspondence: tavassolia@khayam.ut.ac.ir  
School of Chemistry, College of Science, University of Tehran, Tehran  
1513746911, Iran

One of the important factors in catalyst activity and product selectivity is the catalyst preparation method. The synthesis of inorganic nanoparticles is usually carried out in water-in-oil (W/O) microemulsions which consist of small aggregates (micelles) at the microscopic level. W/O microemulsion solutions are mostly transparent isotropic liquid media with nanosized water droplets that are dispersed in the continuous oil phase and stabilized by surfactant molecules at the water/oil interface. These surfactant-covered water pools offer a unique microenvironment for the formation of nanoparticles. In the catalysts prepared by impregnation technique, the structure of the support, especially the pore size, influences the sizes of the formed metal particles with a broad size distribution; while in the catalysts prepared by the microemulsion route, the sizes of the particles will depend on the nature of the microemulsion. In this case, a narrow particle size distribution can be obtained. The main advantages of using the microemulsion technique in the preparation of catalysts is the possibility of controlling properties such as particle size, morphology, and size distribution. Moreover, with the microemulsion method, it is possible to control the composition of the nanoparticles such as bimetallic particles, where the initial ratio of the metal precursor concentrations in the water cores of the micelles will correspond to the final composition of the particles obtained after reduction. Using microemulsion, the bimetallic particle can be formed at room temperature with a true alloy structure; while conventional preparation methods usually require high temperatures which inherently will cause formation of large particles [6-8].

In cobalt-catalyzed Fischer-Tropsch synthesis, to achieve high surface active sites ( $\text{Co}^0$ ), cobalt precursors are dispersed on porous carriers such as  $\text{SiO}_2$ ,  $\text{Al}_2\text{O}_3$ , and to a lesser extent  $\text{TiO}_2$  [9-16]. In our previous works, we showed that a negative aspect of these support materials is their reactivity toward cobalt, which during preparation or catalysis results in the formation of mixed compounds that are reducible only at high reduction temperatures. To avoid these problems, we used the carbon nanotubes (CNTs) as FTS catalyst support. We showed that using CNTs can increase the dispersion of metal clusters and decrease the average cobalt clusters sizes, which in turn can enhance the catalyst performance [4,17-19]. In the mentioned works, we used impregnation method to prepare the carbon nanotubes-supported cobalt catalysts. In the present work, we intend to use the bimetallic microemulsion technique for preparation of ruthenium-promoted cobalt catalyst. Also, the influences of cobalt particle size on the catalyst physicochemical properties, activity, and selectivity were assessed and reported.

## Results and discussion

### Catalysts characterization

The textural properties of the fresh and purified carbon nanotubes are given in the Table 1. The data indicate that in the case of acid-washed support, surface area, total pore volume, and average internal diameter of nanotubes increased significantly which will result in better dispersion of metals as well as enhancement of catalyst activity. Table 1 also shows the Fe content for the untreated fresh CNTs and acid-treated CNTs (determined by ICP). As shown the amount of encapsulated Fe content in the fresh CNTs was about 0.6 wt.% which decreased to 0 for acid-treated CNTs.

Results of surface area measurements for the calcined catalysts are given in the Table 2. These results show that the BET surface areas of the  $\text{C}_4$  to  $\text{C}_8$  (prepared by microemulsion) catalysts are 169 to 187  $\text{m}^2/\text{g}$ . However, the BET surface area for the  $\text{C}_1$  to  $\text{C}_3$  catalysts (prepared by impregnation) is somewhat lower (154 to 158  $\text{m}^2/\text{g}$ ), which indicates some more pore blockage by metal oxide clusters in the catalysts prepared by impregnation method than the catalysts prepared by microemulsion method. This table also shows that the BET surface area of the catalysts prepared by microemulsion increases by decreasing the W/S ratio, indicating smaller cobalt particles and lesser pore blockage by cobalt oxide clusters.

The elemental compositions of the calcined catalysts measured by ICP are given in Table 3. This table shows that the metal contents of the catalysts were fairly similar and close to the targeted metal contents.

Figure 1 presents the TEM image of the purified support. As shown the treated support comprised an interwoven matrix of multiwall CNTs. TEM images of  $\text{C}_4$  catalyst made by the microemulsion method are shown in Figure 2. As shown the very small particles are dispersed mostly inside the tubes and on the outer surface of the CNT walls. The size of the particles located inside and outside the nanotubes are within the range of 2 to 7 nm. The TEM image of  $\text{C}_3$  catalyst prepared by impregnation method is shown in Figure 3. This figure shows that the particles are distributed both inside and outside of the nanotubes walls. The size of particles located inside and outside the nanotubes are within the range of 4–16 nm.

Figure 4 depicts the size distribution of the particles for  $\text{C}_3$  and  $\text{C}_6$  catalysts, which is determined using the population of the total particles of the catalyst based on data taken from five TEM pictures. According to this figure, the average particle size for the  $\text{C}_3$  and  $\text{C}_4$  catalysts are 4.7 and 8.4 nm, respectively. Of particular importance is the particle size distribution which is too narrow in the case of  $\text{C}_3$ , the catalyst prepared by microemulsion method.

**Table 1 Textural properties of the fresh and purified carbon nanotubes**

Sample	BET surface area (m <sup>2</sup> /g)	Total pore volume (ml/g)	Average pore diameter (Å)	Percentage of metal
Fresh CNTs	209	0.48	91.62	0.60
Treated CNTs	252.6	0.59	94.12	0

BET, Brunauer, Emmett, and Teller.

To determine the crystalline phases, XRD of the calcined catalysts were performed. XRD patterns of the catalysts are shown in Figure 5A,B. In the XRD spectra of all the catalysts, the peaks at  $2\theta$  values of  $25^\circ$  and  $43^\circ$  correspond to the support, while the other peaks in the spectra of the catalysts are related to different crystal planes of  $\text{Co}_3\text{O}_4$  [18,19]. The peak at  $36.8^\circ$  is the most intense peak of  $\text{Co}_3\text{O}_4$  in the XRD spectrum of all the catalysts. In the XRD spectrum, no peak of the catalysts was observed in Figure 5A,B due to the low amounts of Ru promoter, indicating diffraction lines of ruthenium oxide. Table 4 shows the average  $\text{Co}_3\text{O}_4$  cluster size of the catalysts calculated from XRD spectrum and Scherrer equation at  $36.8^\circ$  [18]. According to Table 4, the average  $\text{Co}_3\text{O}_4$  cluster size for the catalysts synthesized by microemulsion is significantly lower compared to the catalysts prepared by impregnation method, indicating better dispersion of cobalt clusters. Also in the case of the catalysts prepared by microemulsion, the average  $\text{Co}_3\text{O}_4$  cluster size was decreased from 7.2 to 4.8 nm by decreasing the  $W/S$  ratio from 1.5 to 0.5. The average particle sizes of  $\text{Co}_3\text{O}_4$  are linearly correlated with the water-to-surfactant ratio used during the microemulsion catalyst preparation route. In fact, nanoparticles are formed in the internal structure of the microemulsion, which is determined by the ratio of water to surfactant. At high oil concentration, the bicontinuous phase is transformed into a structure of small water droplets within a continuous oil phase (reverse micelles) when surfactant is added. Thus, the results show that the size of different droplets determines the cobalt's particle size, depending on the amount of surfactant [6-8].

The activation of the catalysts in hydrogen atmosphere was disclosed by TPR experiments. The TPR spectra of the calcined catalysts are shown in Figure 6A,B. In the

TPR profile of all the catalysts, the low temperature peak is typically assigned to reduction of  $\text{Co}_3\text{O}_4$  to  $\text{CoO}$ , although a fraction of the peak likely comprises the reduction of the larger bulk-like  $\text{CoO}$  species to  $\text{Co}^0$  [18,19]. The second broad peak is assigned to the reduction of small  $\text{CoO}$  to  $\text{Co}^0$  species. Figure 6A shows that addition of Ru to the  $\text{Co}/\text{CNTs}$  catalyst decreases the reduction temperature of cobalt oxides significantly. Ruthenium oxide reduces at temperatures lower than the reduction temperature  $\text{Co}_3\text{O}_4$  which in turn enhances the reduction of cobalt oxides by spillover of hydrogen. Figure 6B shows that deposition of cobalt nanoparticles synthesized by microemulsion on the CNTs shifts the reduction peaks of the  $\text{Co}_3\text{O}_4$  to  $\text{CoO}$  and the  $\text{CoO}$  to  $\text{Co}^0$  species to the lower temperatures compared to the catalyst prepared by impregnation method with the same loadings of Co and Ru. Also, for the catalysts prepared by microemulsion, decreasing water-to-surfactant ratio shifts the reduction of the  $\text{Co}_3\text{O}_4$  to  $\text{CoO}$  and the  $\text{CoO}$  to  $\text{Co}^0$  species to the lower temperatures, indicating higher reducibility for the catalysts prepared with lower  $W/S$  ratios. As confirmed by XRD and TEM tests, using microemulsion technique at lower  $W/S$  ratios decreases the cobalt average particle sizes which in turn increases the population of the particles located inside the carbon nanotubes. Positioning the cobalt particles inside the nanotubes favors the reduction of  $\text{Co}_3\text{O}_4$  and  $\text{CoO}$  species. The electron deficiency of the interior CNTs surface is possibly responsible, because the  $\pi$  electron density of the graphene layers shifts from the inner to outer surface of the CNTs. Thus,  $\text{Co}_3\text{O}_4$  should interact with the interior CNT wall differently from that with the exterior wall. This is reflected by the shift of the Co-O vibration mode when  $\text{Co}_3\text{O}_4$  nanoparticles are moved from the outside to the inside of the CNTs channels.

**Table 2 Textural properties of the calcined catalysts with different preparation methods**

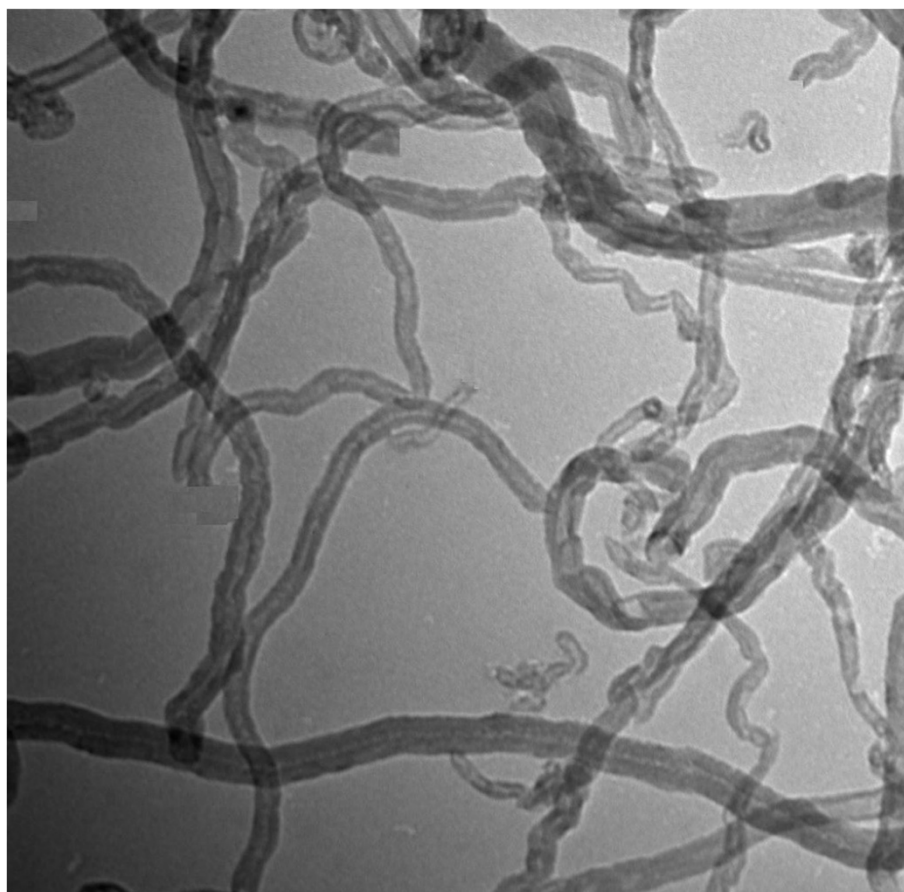
Sample	Preparation route	Co wt.%	Ru wt.%	$W/S$ ratio	BET surface area (m <sup>2</sup> /g)	Total pore volume (ml/g)	Average pore diameter (Å)
C <sub>1</sub>	Impregnation	15	0.0	-	158	0.438	128
C <sub>2</sub>	Impregnation	15	0.5	-	156	0.435	129
C <sub>3</sub>	Impregnation	15	1.0	-	154	0.432	130
C <sub>4</sub>	Microemulsion	15	1.0	0.50	187	0.469	125
C <sub>5</sub>	Microemulsion	15	1.0	0.75	180	0.461	127
C <sub>6</sub>	Microemulsion	15	1.0	1.0	174	0.453	127
C <sub>7</sub>	Microemulsion	15	1.0	1.25	172	0.447	129
C <sub>8</sub>	Microemulsion	15	1.0	1.50	169	0.443	129

**Table 3 Chemical composition of the calcined catalysts**

Catalyst	Targeted composition (wt.%)		Measured composition (wt.%)	
	Co	Ru	Co	Ru
C <sub>1</sub>	15	0.0	14.69	0.0
C <sub>2</sub>	15	0.5	14.68	0.049
C <sub>3</sub>	15	1	14.68	0.979
C <sub>4</sub>	15	1	14.37	0.958
C <sub>5</sub>	15	1	14.40	0.960
C <sub>6</sub>	15	1	14.41	0.961
C <sub>7</sub>	15	1	14.41	0.961
C <sub>8</sub>	15	1	14.43	0.962

Within the channels, the electron density loss can be at least partially compensated through this interaction with the encapsulated  $\text{Co}_3\text{O}_4$ , which can destabilize  $\text{Co}_3\text{O}_4$  and results in an easier reduction. Higher degree of reduction in the case of the catalysts prepared by

microemulsion with lower  $W/S$  ratios will make more cobalt atoms to be available for FTS reaction. Figure 6A, B also indicates that there is no significant evidence of formation of metal-support compounds on the catalyst surface due to the absence of significant reduction peaks



CNT-3-4.tif  
CNT-3-4  
Print Mag: 336000x @ 7.0 in  
14:03 08/06/11  
TEM Mode: Imaging

100 nm  
HV=60.0kV  
Direct Mag: 200000x  
AMT Camera System

**Figure 1** TEM image of the purified CNTs.





15 Co-11.tif

15 Co-11

Print Mag: 577000x @ 8.0 in

11:12 08/06/11

TEM Mode: Imaging

20 nm

HV=60.0kV

Direct Mag: 300000x

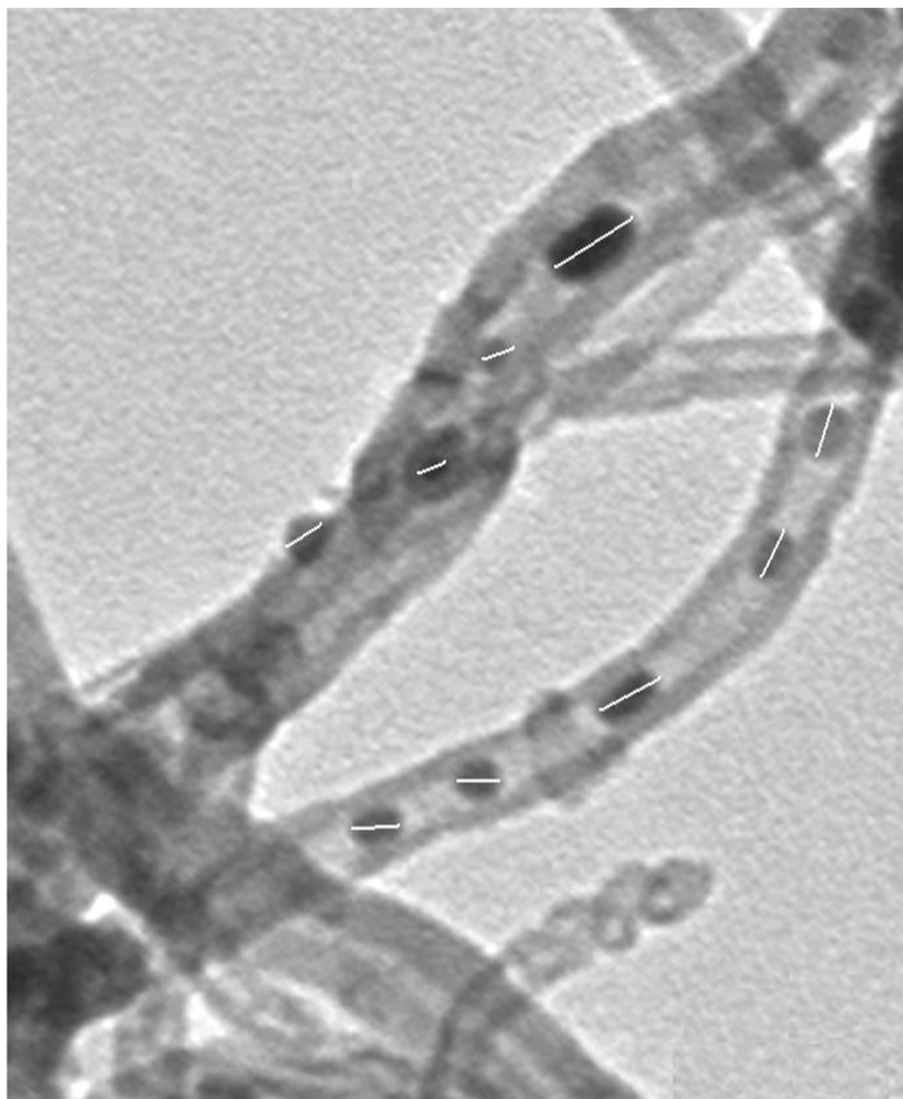
AMT Camera System

**Figure 2** TEM image of the C4 catalyst (prepared by microemulsion and W/S= 0.5).

above 580°C. It has been shown that the reduction peaks present at temperatures above 580°C with oxidic carrier shows formation of cobalt species that are difficult to reduce (oxide compounds). CNTs as an inert support for cobalt catalyst do not show any peak related to formation of metal-support compounds as compared to Co/ $\gamma$ -Al<sub>2</sub>O<sub>3</sub> catalysts, suggesting an easier reduction process with CNTs than with oxidic carriers [17,20].

The results of hydrogen chemisorption tests are given in Table 5. As shown addition of Ru to the unpromoted Co/CNT catalyst increases hydrogen uptake, percentage reduction, and percentage dispersion. Table 5 also shows that using microemulsion considerably increased the

hydrogen uptake and percentage dispersion. For the catalysts prepared with microemulsion method, in accordance with the results of TPR tests, hydrogen uptake and percentage dispersion increased with decreasing W/S ratio. Maximum dispersion is achieved at the minimum W/S ratio of 0.5. The average particle diameter decreased, which are in agreement with the results of XRD and TEM tests. Also, the percentage reduction of the catalysts shows a considerable increase. Higher dispersions and smaller cobalt cluster sizes in the case of the catalysts prepared by microemulsion will increase the number of sites available for CO conversion and hydrocarbon formation reactions rates.



15 Co-12.tif

15 Co-12

Print Mag: 577000x @ 8.0 in

12:31 08/06/11

TEM Mode: Imaging

20 nm

HV=60.0kV

Direct Mag: 300000x

AMT Camera System

**Figure 3** TEM image of the C3 Catalyst (prepared by impregnation).

#### Activity and product selectivity for FTS

The performances of all the catalysts in the Fischer-Tropsch synthesis were tested in a fixed-bed microreactor. All the reactions were performed under a set of standard conditions (220°C, 2 MPa, H<sub>2</sub>:CO = 2). The catalysts reached their normal activity within 24 h. Table 6 presents the FT synthesis rate (g CH/g cat/h), percentage of CO conversion and different product selectivities of the C<sub>4</sub> (prepared by microemulsion 15 wt.% Co and

1 wt.% of Ru) and C<sub>3</sub> (prepared by impregnation 15 wt.% Co and 1 wt.% of Ru) catalysts during the first 24 h of FT synthesis. As shown in Table 6, the FT synthesis productivity of the C<sub>4</sub> catalyst (0.372 g CH/g cat/h) is significantly greater than that of the C<sub>3</sub> catalyst (0.291 g CH/g cat/h). Several reasons can be associated with the improvement in FT synthesis productivity of C<sub>4</sub> catalyst. TEM, XRD, and H<sub>2</sub> chemisorption results showed that the average size of the particles for C<sub>4</sub> and C<sub>3</sub> catalysts

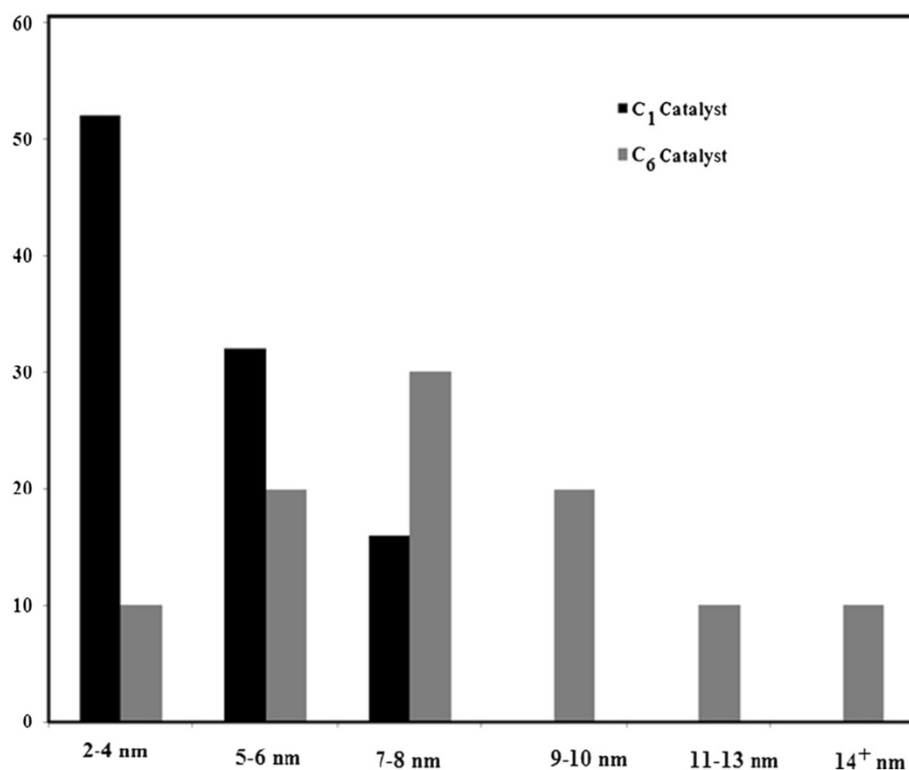


**Figure 4** Particles size distributions for the C<sub>3</sub> and C<sub>4</sub> catalysts.

was about 4.8 and 8.7 nm, respectively. Lower particle sizes in the case of C<sub>4</sub> catalyst increase the active metal surface area which in turn leads to higher FTS rate. As discussed earlier, H<sub>2</sub>-TPR analysis revealed that the reducibility of the C<sub>3</sub> catalyst was higher compared with the C<sub>4</sub>. This phenomenon can result in the formation of more catalytically active sites for FTS. So in industrial scale, using microemulsion method for preparation of FT synthesis catalysts, with higher volumetric productivity, will decrease reactor volume requirements and, as a result, the capital cost of the plant as compared to the catalysts prepared by impregnation.

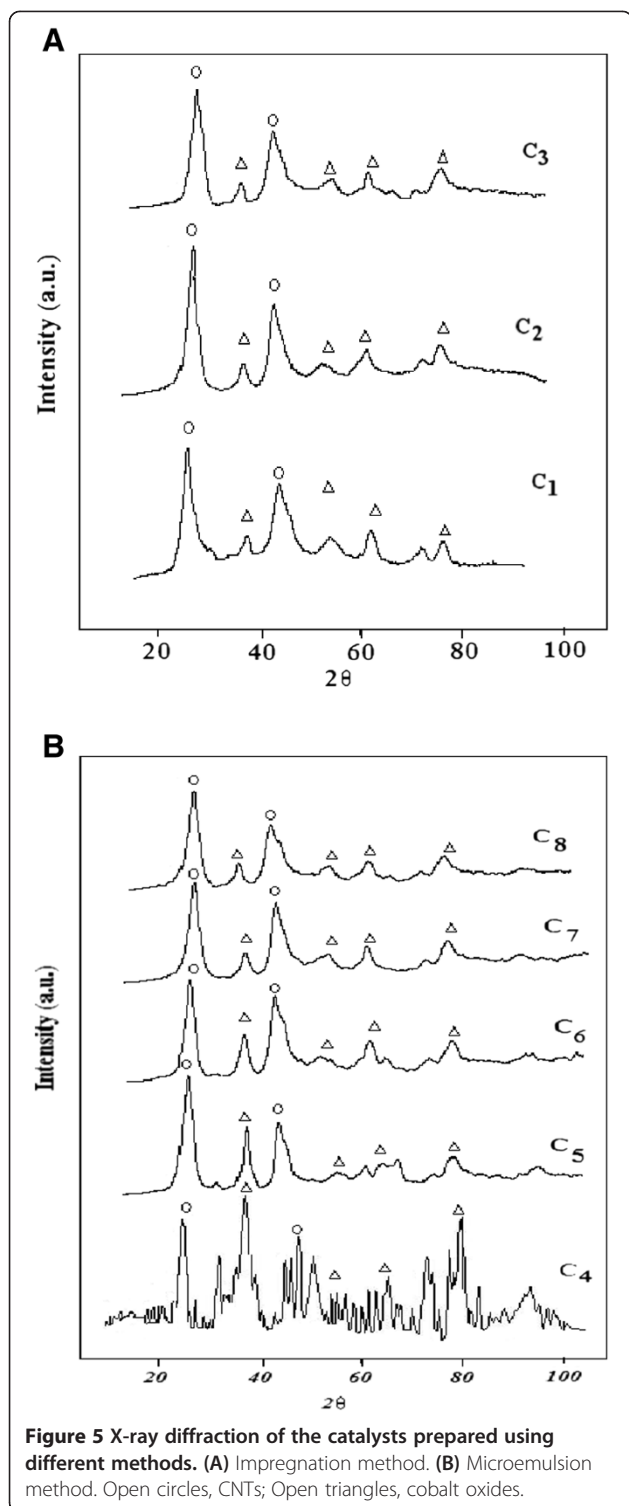
Also the products distribution of C<sub>4</sub> catalyst shows a slight shift to the lower molecular weight hydrocarbons. The data show that CH<sub>4</sub> and light gaseous hydrocarbons selectivities of the C<sub>4</sub> catalyst are about 37.7% higher than that of the C<sub>3</sub> catalyst. Also C<sub>5</sub><sup>+</sup> selectivity of the C<sub>4</sub> is about 5.44% lower than that of the C<sub>3</sub>. CO<sub>2</sub> selectivities of the C<sub>3</sub> and C<sub>4</sub> catalysts are comparable, indicating similar water-gas shift activity for both catalysts. It seems that confinement of the cobalt particles inside the pores in the case of C<sub>3</sub> catalyst can restrain the growth of longer chain hydrocarbons. The inner sides of the CNTs are electron deficient and can restrain the dissociative adsorption of CO and readsorption of olefins resulting in production of lower chain hydrocarbons for C<sub>3</sub> catalyst. The result of Table 6 shows that C<sub>4</sub>-

catalyzed FT synthesis is advantageous in carbon utilization as compared to processes using C<sub>3</sub> catalyst. It worthy is to note that the microemulsion preparation method is more expensive than the impregnation method.

Figure 7 shows the variations of percentage of CO conversion and the number of active cobalt sites with water-to-surfactant ratio for the catalysts prepared by impregnation and different amounts of Ru. Number of active cobalt sites was defined as:

$$\text{No. act. site} = \text{Wt. of Co} \times \text{red. frac.} \times \text{Dis} \times N_A \times \text{MW},$$

where  $N_A$  is Avogadro's number and MW is molecular weight of cobalt. As shown on this figure, addition of Ru to the unpromoted cobalt catalyst increases the number of active cobalt sites as well as the percentage of CO conversion. The trend for the percentage of CO conversion is similar to that for the number of active cobalt sites. The percentage of CO conversion increases in accordance with the number of active cobalt sites. The maximum FTS activity is achieved with the maximum amount of Ru and highest number of active cobalt sites. TPR and H<sub>2</sub> chemisorption tests showed that addition of Ru to the unpromoted cobalt catalyst increases the percentage reduction of the catalyst. This figure reveals that



the Fischer-Tropsch activity is strongly proportional to the number of surface-reduced cobalt sites. Therefore, the maximum concentration of surface  $\text{Co}^{\circ}$  sites and FTS activity is achieved for the  $\text{C}_3$  catalyst, presenting the highest dispersion and highest reducibility. Figure 8 shows the methane, light gaseous hydrocarbons, and  $\text{C}_5^+$

**Table 4 Particle sizes of the calcined catalysts with different preparation methods**

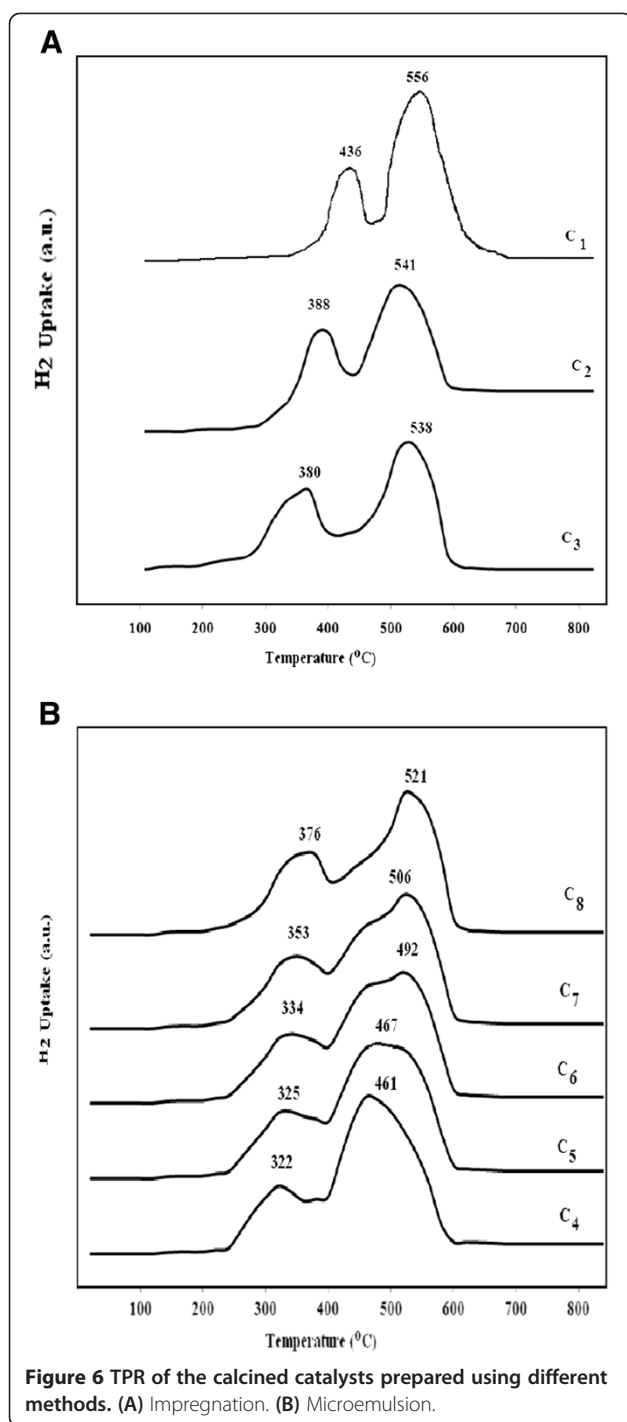
Catalyst	$d (\text{Co}_3\text{O}_4)$ (nm) calculated by Debye-Scherrer formula
$\text{C}_1$	8.5
$\text{C}_2$	8.6
$\text{C}_3$	8.7
$\text{C}_4$	4.8
$\text{C}_5$	5.0
$\text{C}_6$	5.3
$\text{C}_7$	5.7
$\text{C}_8$	7.2

selectivities of the  $\text{C}_1$  to  $\text{C}_3$  catalysts. As shown the methane and light gaseous hydrocarbon selectivities are reduced with increasing Ru. The catalyst prepared with 1 wt.% of Ru showed lowest selectivity to methane. The  $\text{C}_5^+$  selectivity is increased with increasing Ru. Ruthenium enriches on the surface and since Ru is the most selective FTS catalysts towards higher molecular weight hydrocarbons, enhances the selectivity of unpromoted Co/CNTs toward higher molecular weight hydrocarbons.

Figure 9 shows the variations of percentage of CO conversion and the number of active cobalt sites with water-to-surfactant ratio for the catalysts prepared by microemulsion. This figure also reveals that increasing the water-to-surfactant ratio decreases the number of active cobalt sites. The trend for the percentage of CO conversion is similar to that for the number of active cobalt sites. The percentage of CO conversion decreases in accordance with the number of active cobalt sites. The maximum FTS activity is achieved with the minimum W/S ratio and highest number of active cobalt sites. This figure reveals that the Fischer-Tropsch activity is strongly proportional to the number of surface-reduced cobalt sites. Therefore, the maximum concentration of surface  $\text{Co}^{\circ}$  sites and FTS activity is achieved for the  $\text{C}_4$  catalyst, presenting the lowest average cobalt particle sizes, best dispersion, and highest reducibility. Also, improvement of the uniformity of the catalyst particles by decreasing the W/S ratio leads to a better stability of the products and the FTS activity.

Figure 10 shows the methane, light gaseous hydrocarbons, and  $\text{C}_5^+$  selectivities of the catalysts with variation of W/S ratio. As shown the methane and light gaseous hydrocarbon selectivities are reduced with increasing W/S ratio. The catalyst prepared with W/S of 1.5 showed the lowest selectivity to methane. The  $\text{C}_5^+$  selectivity is increased with increasing W/S ratio. The Anderson-Schultz-Florey (ASF) model is a common model used to describe the chain growth mechanism in FTS. According to this model, the polymerization process in FTS is assumed to initiate on the surface of the catalyst by a





monomer that contains one carbon atom. Chain growth takes place by the addition of monomers to the growing chains. It seems that the steric hindrance for dissociative adsorption of CO and formation of CH<sub>2</sub> monomer and addition of this monomer to the growing chain is less in the larger cobalt clusters which are formed at low W/S ratios.

## Experimental

### Catalyst preparation

Multiwall CNTs (characteristics are shown in Table 1) were used as support for preparation of the catalysts. Prior to catalyst preparation, the support was treated with 30% HNO<sub>3</sub> refluxed at 120°C overnight, washed with distilled water several times, and dried at 120°C for 6 h. Two different sets of catalysts were prepared by microemulsion and impregnation methods. For the first set of the catalysts, the concentration of cobalt was adjusted at 15 wt.% and the concentrations of ruthenium were adjusted at 0.0, 0.5, and 1.0 wt.%. The catalysts were prepared by the co-impregnation method using aqueous solutions of CO(NO<sub>3</sub>)<sub>2</sub>·6H<sub>2</sub>O and Ru(NO)(NO<sub>3</sub>)<sub>3</sub>. After the impregnation step, the catalysts were dried at 120°C and calcined at 450°C under argon flow for 3 h and slowly exposed to an oxygen atmosphere during the cooling step. The catalysts prepared by this procedure were signified as C<sub>1</sub>, C<sub>2</sub>, and C<sub>3</sub> (see Table 2).

For the second set of the catalysts, the concentrations of cobalt and ruthenium were fixed at 15 and 1 wt.%, respectively. The catalysts were prepared by microemulsion technique with aqueous solutions of cobalt nitrate [CO(NO<sub>3</sub>)<sub>2</sub>·6H<sub>2</sub>O%99, Merck] (Whitehouse Station, NJ, USA) and ruthenium nitrosil nitrate [Ru(NO)(NO<sub>3</sub>)<sub>3</sub>] (Sigma-Aldrich, St. Louis, MO, USA). Ruthenium-promoted cobalt nanoparticles were synthesized in a reverse microemulsion using a nonionic surfactant Triton X-100 (Chem-Lab, Fisher Scientific, Loughborough, Leicestershire, UK), *n*-hexane [C<sub>6</sub>H<sub>14</sub>] (Chem-Lab) as the oil phase and 1-butanol [C<sub>4</sub>H<sub>9</sub>OH] (Merck) as the co-surfactant. The water-to-surfactant molar ratio (W/S) was varied from 0.5 to 1.5. After vigorous stirring, a microemulsion was obtained (15 min). Hydrazine was added in excess (hydrazine/Co = 10) to improve nanoparticle formation in the core of the micelles by reducing the metal oxides. Then, the appropriate weight of purified carbon nanotubes was added under stirring. During 3 h of stirring, tetrahydrofuran (THF), an emulsion destabilizing agent, was added dropwise (1 ml/min). A fast addition could lead to fast particle agglomeration and uncontrolled particle deposition on the support (CNTs). The mixture was left to mature and settle slowly overnight and then decanted. The solid sample was recovered by vacuum filtration using ashless filtration paper (Whatman 1; Whatman plc, Maidstone, Kent, UK) and washed several times with distilled water ethanol. In order to remove the remaining traces of surfactant and ammonia, the catalysts were dried at 120°C for 2 h and calcined under argon (Ar) flow at 450°C for 3 h and slowly exposed to an oxygen atmosphere during the cooling step. The catalysts prepared by this procedure were signified as C<sub>4</sub>, C<sub>5</sub>, C<sub>6</sub>, C<sub>7</sub>, and C<sub>8</sub> for a W/S ratio of 0.50, 0.75, 1, 1.25, and 1.50, respectively (see Table 2).

**Table 5 H<sub>2</sub> chemisorption results for the calcined catalysts with different preparation methods**

Catalyst	Micromole of H <sub>2</sub> desorbed/ g cat	Micromole of O <sub>2</sub> consumed/ g cat	Percentage of reduction	Percentage of dispersion	d (Co <sub>3</sub> O <sub>4</sub> ) (nm)	d (Co <sup>0</sup> ) (nm)
C <sub>1</sub>	210	697	36.1	13.45	8.1	6.1
C <sub>2</sub>	220	840	43.6	14.10	8.3	6.2
C <sub>3</sub>	226	865	44.9	14.50	8.5	6.4
C <sub>4</sub>	393	1,265	65.7	26.75	4.6	3.5
C <sub>5</sub>	374	1,195	62.1	25.30	4.9	3.7
C <sub>6</sub>	339	1,127	58.5	22.80	5.4	4.1
C <sub>7</sub>	312	1,040	54.0	20.50	5.9	4.4
C <sub>8</sub>	259	921	47.8	16.60	7.1	5.3

#### Inductively coupled plasma-optical emission spectrometry

The metal loadings of the calcined catalysts were performed using Varian VISTA-MPX inductively coupled plasma-optical emission spectrometry (ICP-OES) instrument (Varian Medical Systems, Inc., Palo Alto, CA, USA).

#### Brunauer, Emmett, and Teller surface area measurements/Barrett-Joyner-Halenda pore size distributions

Surface area, pore volume, and average diameter of pores of the calcined catalysts were measured using an ASAP-2010 V2 Micromeritics system (Micromeritics Instrument Corp., Norcross, GA, USA). The samples were degassed at 200°C for 4 h under 50 mTorr vacuums and their Brunauer, Emmett and Teller (BET) area, pore volume, and pore diameter were determined.

#### Transmission electron microscopy

The morphology of the treated CNTs and C<sub>3</sub> and C<sub>4</sub> catalysts was studied by transmission electron microscopy (TEM). Sample specimens for TEM studies were prepared by ultrasonic dispersion of the catalysts in ethanol, and the suspensions were dropped onto a carbon-coated copper grid. TEM investigations were carried out using a Philips CM20 (100 kV) transmission electron microscope equipped with a NARON energy-dispersive spectrometer with a germanium detector (Philips, Amsterdam, The Netherlands).

#### X-ray diffraction

The phases and particle sizes of the crystals present in the catalysts were analyzed by X-ray diffraction (XRD) experiments using a Philips analytical X-ray diffractometer (XPert MPD) with monochromatized Cu/Kα

radiation, 2θ angles from 20° to 80°. The Debye-Scherrer formula was applied to Co<sub>3</sub>O<sub>4</sub> peaks at 2θ = 36.8, in order to calculate the average particle sizes.

#### Temperature-programmed reduction

The H<sub>2</sub>-TPR profiles of the catalysts were performed in order to study the reducibility of the metal species in the catalysts. The calcined catalyst sample (0.05 g) was first purged in a flow of Helium at 140°C to remove traces of water and gases exist in catalyst, and then cooled to 40°C. Then the temperature-programmed reduction (TPR) of each sample was performed using 5% H<sub>2</sub> in Ar stream at a flow rate of 40 ml/min at atmospheric pressure using Micromeritics TPD-TPR 2900 analyzer equipped with a thermal conductivity detector (TCD), heating at a linearly programmed rate of 10°C/min up to 850°C.

#### Hydrogen chemisorption

The amount of chemisorbed hydrogen on the catalysts was measured using the Micromeritics TPD-TPR 290 system. Sample amount of 0.25 g was reduced under hydrogen flow at 400°C for 12 h and then cooled to 100°C under hydrogen flow. Then the flow of hydrogen was switched to argon at the same temperature, which lasted about 30 min in order to remove the weakly adsorbed hydrogen. Afterwards, the temperature-programmed desorption (TPD) of the samples was obtained by increasing the temperature of the samples, with a ramp rate of 10°C/min, to 400°C under the argon flow. The TPD profile was used to determine the cobalt dispersion and its surface average crystallite size. After the TPD of hydrogen, the sample was reoxidized at 400°C by pulses of 10% oxygen in helium to determine the extent of reduction. It is assumed that Co<sup>0</sup> is oxidized to Co<sub>3</sub>O<sub>4</sub>. The calculations are summarized below:

**Table 6 FT synthesis results during first 24 h for the C<sub>3</sub> and C<sub>4</sub> catalysts**

Catalyst	Percentage of CO conversion	FTS rate (g CH/g cat/h)	CO <sub>2</sub> selectivity	CH <sub>4</sub> selectivity	C <sub>2</sub> -C <sub>4</sub> selectivity	C <sub>3</sub> <sup>+</sup> selectivity
C <sub>4</sub>	75.05	0.372	0.510	7.97	3.91	87.61
C <sub>3</sub>	59.09	0.291	0.51	4.68	2.43	92.38

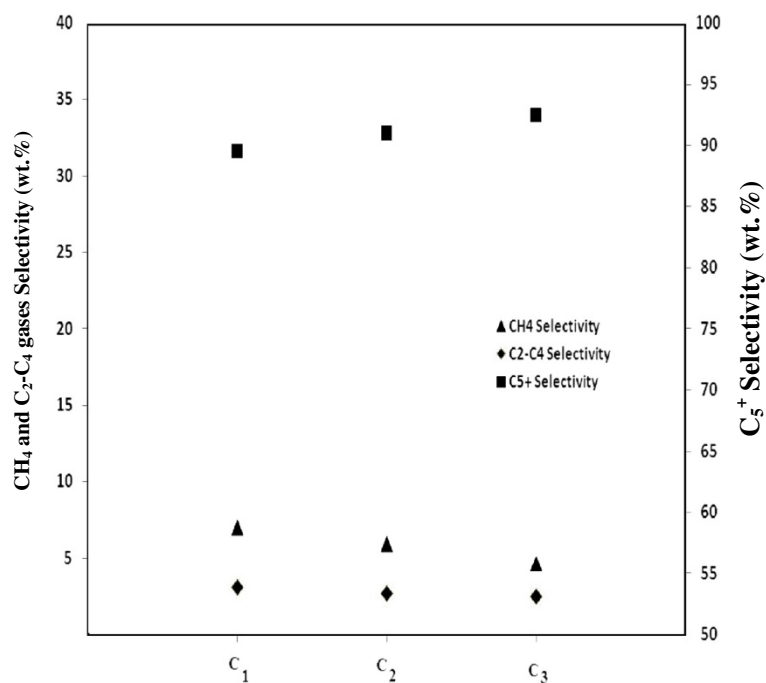


**Figure 7** Variations of percentage of CO conversion and number of active cobalt sites for the catalyst prepared with impregnation.

$$\text{Calibration value (l gas/area units)} = \frac{\text{Loop volume} \times \% \text{ Analytical gas}}{\text{Mean calibration area} \times 100} \quad (1)$$

$$\text{H}_2 \text{ uptake (moles/g}_{\text{cat}}) = \frac{\text{Analytical area from TPD} \times \text{Calibration value}}{\text{Sample weight} \times 24.5} \quad (2)$$

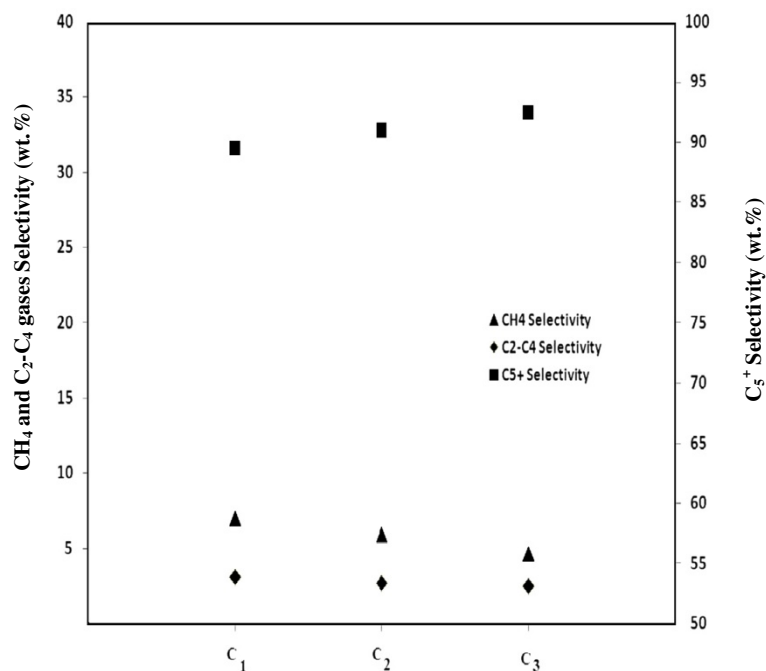


**Figure 8** Variations of CH<sub>4</sub>, C<sub>2</sub> to C<sub>4</sub>, and C<sub>5</sub><sup>+</sup> selectivities for the catalyst prepared with impregnation.

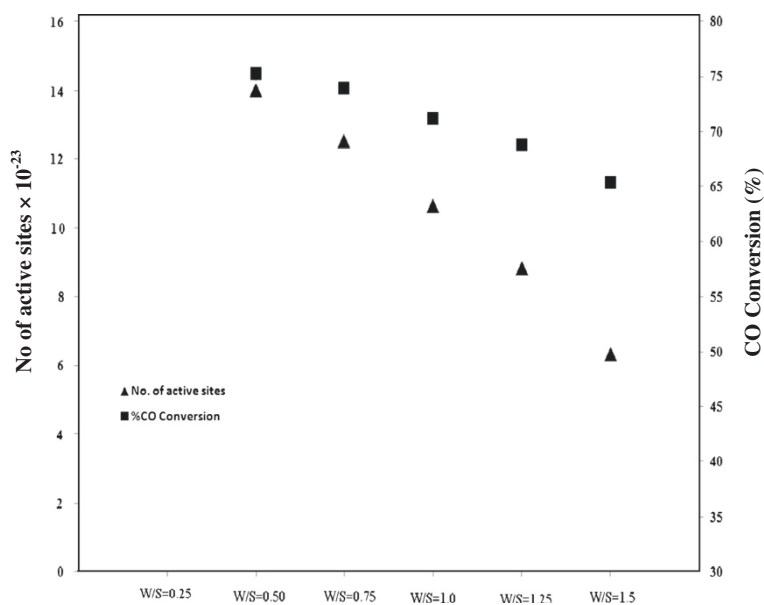


Figure 9 Variations of the percentage of CO conversion and number of active cobalt sites with water-to-surfactant ratio.

$$\%D_{\text{Total Co}} = \frac{\text{H}_2 \text{ uptake} \times \text{Atomic weight} \times \text{Stoichiometry}}{\text{Number of Co}^0 \text{ atoms on the surface} \times 100} \times 100$$

$$= \frac{\% \text{ Metal}}{\text{Total number of Co}^0 \text{ atom}} \times 100$$

(3)

$$\text{O}_2 \text{ uptake (moles/g}_{\text{cat}}) = \frac{\text{Sum of consumed pulse areas} \times \text{Calibration value}}{\text{Sample weight} \times 24.5}$$

(5)

$$\%D_{\text{reduced Co}} = \frac{\text{Number of Co}^0 \text{ atoms on the surface} \times 100}{\text{Total number of Co}^0 \text{ atom} \times \text{Reduced fraction}}$$

(4)

$$\text{Reduced fraction} = \frac{\text{O}_2 \text{ uptake (moles/g cat)} \times 2/3 \times \text{Atomic weight}}{\% \text{ Metal}}$$

(6)

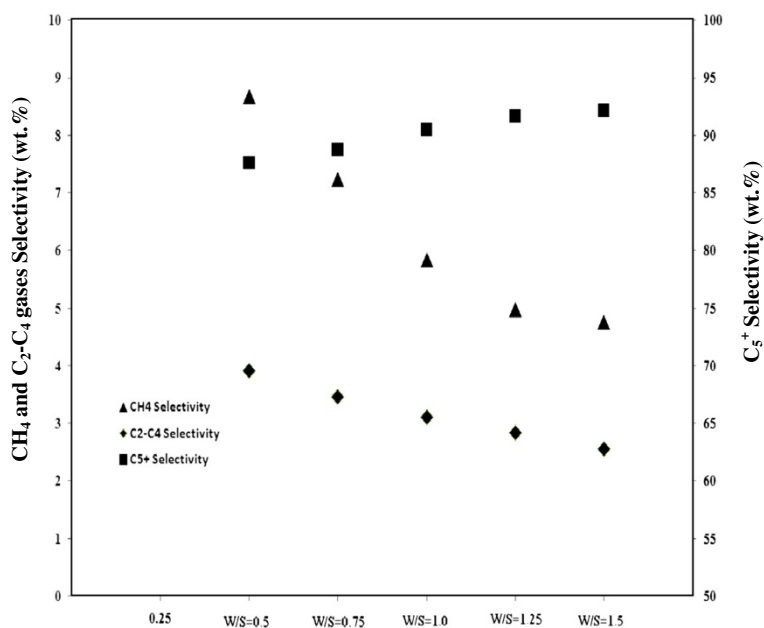


Figure 10 Variations of CH<sub>4</sub>, C<sub>2</sub> to C<sub>4</sub>, and C<sub>5</sub><sup>+</sup> selectivities with water-to-surfactant ratio.

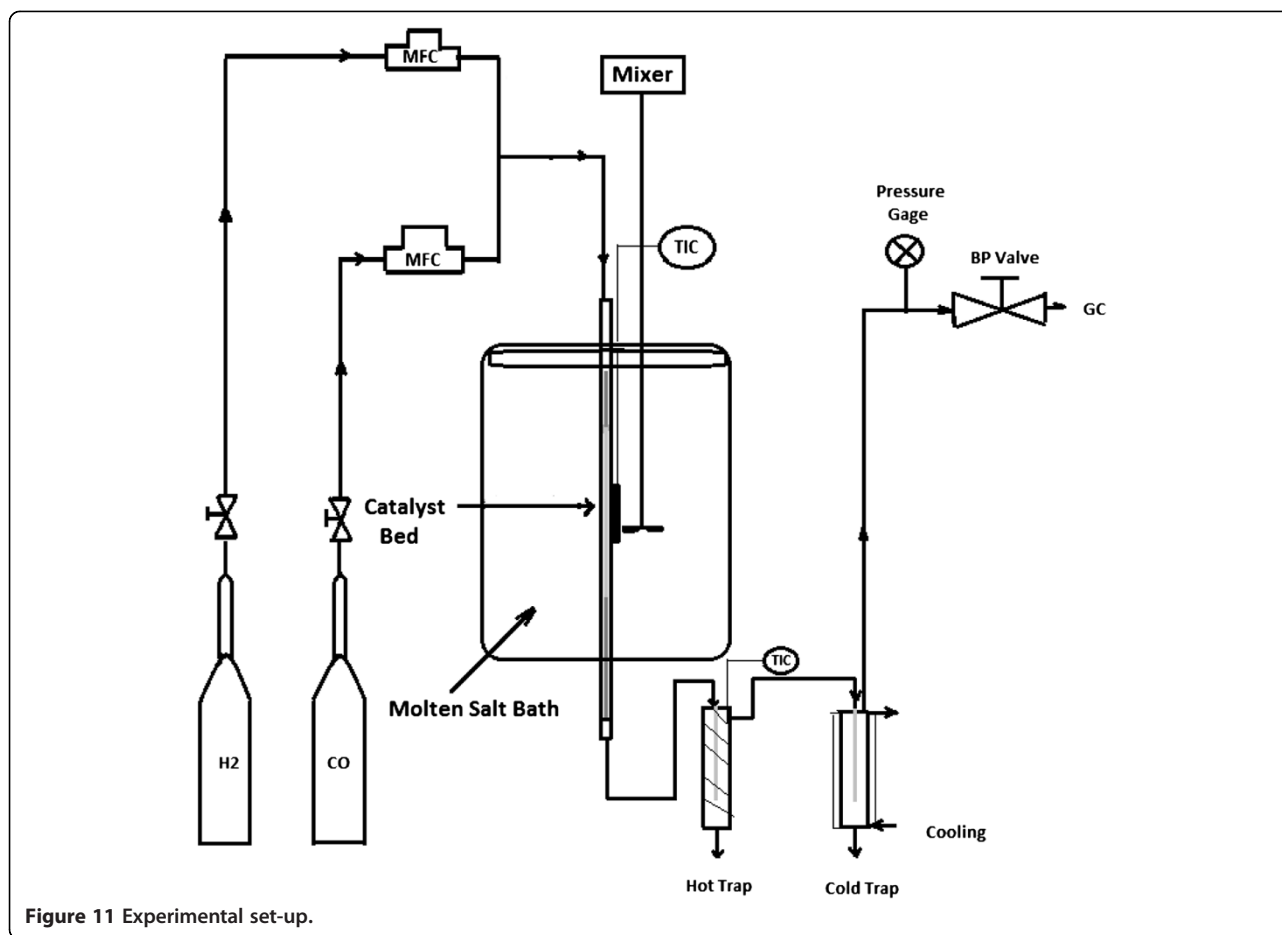


Figure 11 Experimental set-up.

$$\text{Diameter (nm)}_{\text{total Co}} = \frac{6,000}{\text{Density} \times \text{Maximum area} \times \text{Dispersion}} \quad (7)$$

$$\text{Diameter (nm)}_{\text{reduced Co}} = \frac{6,000}{\text{Density} \times \text{Maximum area} \times \text{Dispersion} \times \text{Reduced fraction}} \quad (8)$$

### Reaction testing

Fischer-Tropsch synthesis has been performed in a tubular down flow, fixed-bed reactor system. Figure 11 shows the experimental setup. The reactor was made up of stainless steel tube of 450-mm length and 22-mm inside diameter. Brooks' 5850 mass flow controllers were used to add H<sub>2</sub> and CO at the desired rate to the reactor. Typically, 1 g of the catalyst was charged into the reactor. The reactor was placed in a molten salt bath with a stirrer to ensure a uniform temperature along the

catalytic bed. The bath temperature was controlled via a PID temperature controller. The catalyst was reduced under hydrogen flow at 400°C for 12 h. After the catalyst reduction, the mixed gases (CO and H<sub>2</sub>) were fed at a flow of 50 ml/min, a temperature of 220°C, H<sub>2</sub>/CO ratio of 2, and pressure of 2 MPa. The products were continuously removed from the reactor and passed through two traps, one maintained at 100°C (hot trap) and the other at 0°C (cold trap). The CO, CO<sub>2</sub>, and other gaseous products were monitored with time intervals of 2 h. The liquid products were collected after completion of the run and analyzed by means of three gas chromatographs, a Shimadzu 4C gas chromatograph (Shimadzu Corp., Kyoto, Japan) equipped with two subsequently connected packed columns: Porapak Q (Sigma-Aldrich Corp., St. Louis, MO, USA) and molecular sieve 5 Å, and a TCD with argon which was used as a carrier gas for hydrogen analysis. A Varian CP 3800 with a Petrocol Tm DH100 fused silica capillary column (Sigma-Aldrich Corp., St. Louis, MO, USA) and a flame ionization detector (FID) were used for liquid products so that a



complete product distribution could be provided. A Varian CP 3800 with a chromosorb column and a TCD were used for CO, CO<sub>2</sub>, CH<sub>4</sub>, and other noncondensable gases.

## Conclusions

Ruthenium-promoted cobalt nanocatalysts that are supported by carbon nanotubes (CNTs) are prepared using microemulsion technique with water-to-surfactant ratios of 0.5 to 1.5 and their physicochemical properties and performance in FTS have been assessed and were compared with the catalyst prepared by impregnation method. Ruthenium increased the percentage reduction of the unpromoted catalyst by a factor of 25%. Very narrow particle size distribution has been produced by the microemulsion technique at the relatively high loadings of active metals (15 wt.% Co and 1 wt.% of Ru). Addition of ruthenium increased the percentage conversion and C<sub>5</sub><sup>+</sup> selectivity of the unpromoted catalyst by a factor of 22.6% and 7%, respectively. Using microemulsion technique with water-to-surfactant ratio of 0.5 decreased the average cobalt oxide particle sizes to 4.8 nm. The dispersion percentage is almost doubled and the reduction percentage increased by 28. Activity and selectivity were found to be dependent on the catalyst preparation method and cobalt average particle sizes. The percentage of CO conversion and FTS rate increased from 59.09 to 75.05 and 0.291 to 0.372 gr HC/gr cat/h, respectively, while the C<sub>5</sub><sup>+</sup> liquid hydrocarbons selectivity decreased slightly.

## Competing interest

The authors declare that they have no competing interests.

## Authors' contribution

AT: Writing paper, Guidance. ST: testing in laboratory. ST and SK: making set up. All authors read and approved the final manuscript.

## Authors' information

Ahmad Tavasoli: professor, university of Tehran. Somaye Taghavi: master student, university of Tehran. Saber Tabyar: master student. Saba karimi: master of student, university of Tehran.

Received: 8 December 2012 Accepted: 3 November 2013

Published: 02 Jan 2014

## References

1. Dry ME (2002) The Fischer-Tropsch process. *Catal Today* 71:227–241
2. Van Der Laan GP, Beenackers A (2000) *Appl Catal A* 193:39–53
3. Iglesia E (1997) Design, synthesis, and use of cobalt-based Fischer-Tropsch synthesis catalysts. *Appl Catal A* 161:59–78
4. Trepanier M, Tavasoli A, Dalai AK, Abatzoglou N (2009) Co, Ru and K loadings effects on the activity and selectivity of carbon nanotubes supported cobalt catalyst in Fischer-Tropsch synthesis. *Appl Catal A* 353:193–202
5. Jacobs G, Das TK, Zhang Y, Li J, Racoillet G, Davis BH (2002) Fischer-Tropsch synthesis: support, loading, and promoter effects on the reducibility of cobalt catalysts. *Appl Catal A* 233:263–281
6. Eriksson S, Nylén U, Rojas S, Boutonnet M (2004) Preparation of catalysts from microemulsions and their applications in heterogeneous catalysis. *Appl Catal A* 265:207–219
7. Paul BK, Moulik SP (1997) Microemulsions: an overview. *Dispersion Sci Tech* 18:301–367
8. Boutonnet M, Lögdberg S, Svensson EE (2008) Recent developments in the application of nanoparticles prepared from w/o microemulsions in heterogeneous catalysis. *Curr Opin Colloid Interface Sci* 13:270–286
9. Jacobs G, Das TK, Zhang Y, Li J, Racoillet G, Davis BH (2002) Fischer-Tropsch synthesis: support, loading, and promoter effects on the reducibility of cobalt catalysts. *Appl Catal A Gen* 233:263–281
10. Berge VPJ, van de Loosdrecht J, Barradas S, van der Kraan AM (2000) Oxidation of cobalt based Fischer-Tropsch catalysts as a deactivation mechanism. *Catal Today* 58:321–334
11. Reuel RC, Bartholomew CH (1984) Effects of support and dispersion on the CO hydrogenation activity/selectivity properties of cobalt. *J Catal* 85:78–88
12. Das TK, Jacobs G, Patterson PM, Conner WA, Li J, Davis BH (2003) Fischer-Tropsch synthesis: characterization and catalytic properties of ruthenium promoted cobalt alumina catalysts. *Fuel* 82:805–815
13. Martinez A, Prieto G (2007) Breaking the dispersion-reducibility dependence in oxide-supported cobalt nanoparticles. *J Catal* 245:245–470
14. Bechera R, Balloy D, Vanhove D (2001) Catalytic properties of Co/Al<sub>2</sub>O<sub>3</sub> system for hydrocarbon synthesis. *Appl Catal A* 207:343–353
15. Elbasher NO, Roberts CB (2005) Enhanced incorporations of  $\alpha$ -olefins in the Fischer-Tropsch synthesis chain-growth process over an alumina supported cobalt catalysts in near-critical and supercritical hexane medium. *Ind Eng Chem Res* 44:505–521
16. Tavasoli A, Mortazavi Y, Khodadadi A, Sadagiani K (2005) Effects of different loadings of Ru and Re on physico-chemical properties and performance of 15% Co/Al<sub>2</sub>O<sub>3</sub> FTS catalysts. *Iranian J Chem Chem Eng* 35:9–15
17. Tavasoli A, Sadaghiani K, Nakhaeipour A, Ghalbi Ahangari M (2007) Cobalt loading effects on the structure and activity for Fischer-Tropsch and water-gas shift reactions of Co/Al<sub>2</sub>O<sub>3</sub> catalysts. *IJCE* 29:1–12
18. Tavasoli A, Malek Abbaslou R, Trepanier M, Dalai AK (2008) Fischer-Tropsch synthesis over cobalt catalyst supported on carbon nanotubes in a slurry reactor. *Appl Catal A* 345:134–142
19. Tavasoli A, Sadagiani K, Khorashe F, Seifkordi AA, Rohania AA, Nakhaeipour A (2008) Cobalt supported on carbon nanotubes - a promising novel Fischer-Tropsch synthesis catalyst, fuel processing tech. 89:491–498
20. Chen W, Fan Z, Pan X, Bao X (2008) Effect of confinement in carbon nanotubes on the activity Fischer-Tropsch iron catalysts. *J Am Chem Soc* 130:9414–9419

10.1186/2228-5547-5-1

Cite this article as: Tavasoli et al.: Enhancement of ruthenium-promoted Co/CNT nanocatalyst performance using microemulsion technique. *International Journal of Industrial Chemistry* 2014, 5:1

Submit your manuscript to a SpringerOpen® journal and benefit from:

- Convenient online submission
- Rigorous peer review
- Immediate publication on acceptance
- Open access: articles freely available online
- High visibility within the field
- Retaining the copyright to your article

Submit your next manuscript at ► [springeropen.com](http://springeropen.com)